

Identification of Short Hydrophobic Cell-Penetrating Peptides for Cytosolic Peptide Delivery by Rational Design

Samuel Schmidt,[§] Merel J. W. Adjobo-Hermans,[§] Robin Kohze,[§] Thilo Enderle,[†] Roland Brock,[§]^{ID} and Francesca Milletti^{*,‡}

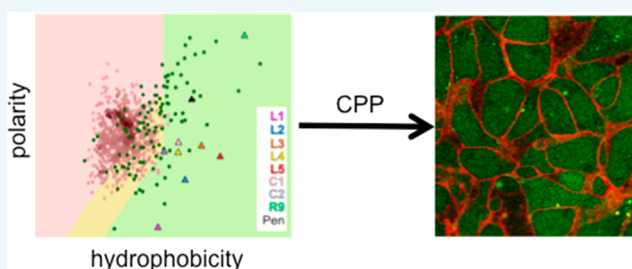
[§]Department of Biochemistry (286), Radboud Institute for Molecular Life Sciences, Radboud University Medical Center, Geert Grooteplein 28, 6525 GA Nijmegen, The Netherlands

[†]Roche Pharmaceutical Research and Early Development, Roche Innovation Center Basel, Grenzacherstrasse 124, 4070 Basel, Switzerland

[‡]Roche Pharmaceutical Research and Early Development, Roche Innovation Center New York, 430 East 29th Street, 10016 New York, New York, United States

Supporting Information

ABSTRACT: Cell-penetrating peptides (CPPs) enhance the cellular uptake of membrane-impermeable molecules. Most CPPs are highly cationic, potentially increasing the risk of toxic side effects and leading to accumulation in organs such as the liver. As a consequence, there is an unmet need for less cationic CPPs. However, design principles for effective CPPs are still missing. Here, we demonstrate a design principle based on a classification of peptides according to accumulated side-chain polarity and hydrophobicity. We show that in comparison to randomly selected peptides, CPPs cover a distinct parameter space. We designed peptides of only six to nine amino acids with a maximum of three positive charges covering this property space. All peptides were tested for cellular uptake and subcellular distribution. Following an initial round of screening we enriched the collection with short and hydrophobic peptides and introduced D-amino acid substitutions and lactam bridges which increased cell uptake, in particular for long-term incubation. Using a GFP complementation assay, for the most active peptides we demonstrate cytosolic delivery of a biologically active cargo peptide.



INTRODUCTION

Cell-penetrating peptides (CPPs) hold great promise as vectors to yield cellular entry of charged (macromolecular) molecules that otherwise do not cross the plasma membrane. In most cases conjugation has been achieved through covalent coupling, but for charged oligonucleotides, noncovalent polyplexes are used preferentially. CPPs are about 5 to 30 amino acids long, and can be subdivided into different classes based on the properties of the amino acid side chains.¹ Even though most CPPs are positively charged, and arginines result in better uptake than lysines, noncharged residues are also crucial for peptide uptake. In addition, the specific sequence can also play a role.² For penetratin, activity depends on the presence of tryptophan residues that are believed to promote interactions with lipid bilayers.^{3,4} For arginine-rich CPPs, one long stretch of arginine residues is more effective than two spatially separated domains of the same total length.⁵

The prototypic arginine-rich CPPs nonaarginine and Tat, and the amphipathic penetratin peptide are among the most effective and widely used CPPs. However, their large number of positive charges poses toxicity concerns, particularly for CPP development as therapeutics.^{6,7} Highly hydrophobic peptides

such as the so-called membrane translocating sequence tend to have poor solubility and to aggregate in aqueous solution.^{8,9}

Hallbrink et al. have shown that peptide bulk properties based on amino acid descriptors can be used to predict CPPs.¹⁰ This analysis employed a five-dimensional parameter set and focused on a scanning of transmembrane proteins for domains with CPP activity.¹¹

Here, we set out to identify short peptides with minimal total charge. This search was based on a parametrization of peptides according to accumulated side-chain properties with respect to only two dimensions, polarity and hydrophobicity. We focused on the application of peptides in the delivery of small molecules and peptides. For delivery of negatively charged oligonucleotides, the capacity to form noncovalent polyplexes constitutes an additional structure–activity relationship, and therefore these peptides should be considered as a class of their own.¹²

As a model cargo we employed a 16-amino-acids peptide corresponding to the 11th strand of the green fluorescent protein β -barrel. In cells expressing the GFP1–10 fragment,

Received: September 17, 2016

Revised: November 22, 2016

Published: November 28, 2016

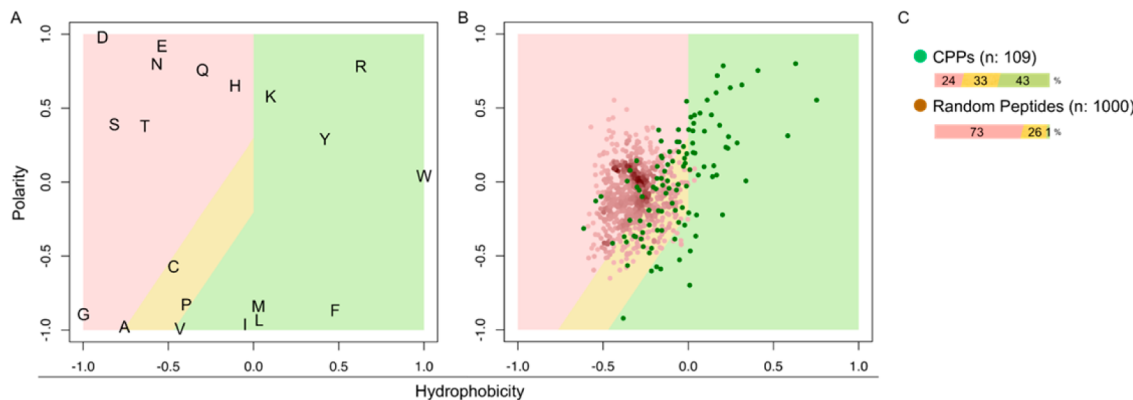


Figure 1. (A) Principal properties of amino acid side chains. The green area was defined based on the largest enrichment of CPPs versus random peptides (43% vs 1%); the yellow and red areas correspond to medium and low prevalence of CPPs, respectively. (B) Coverage of the property space by cell-penetrating versus random peptides and (C) fraction of peptides belonging to each class.

cytosolic delivery of this peptide leads to formation of fluorescent GFP following binding of the cargo to GFP1–10. This reporter assay works with micromolar sensitivity.^{13,14}

By testing two consecutive collections of peptides in three different cell lines and for various times of incubation we identified CPPs with only 6 to 8 amino acids in length and only two positively charged residues that yield delivery and GFP complementation. In particular for long-term incubation, the incorporation of individual D-amino-acids and a lactam bridge increased uptake efficiency.

RESULTS

Physicochemical Properties of Cell-Penetrating Peptides. The broad sequence diversity of cell-penetrating peptides has thwarted efforts to understand cellular uptake based on structure–activity relationships. However, CPPs differ from most peptides based on their amino acid composition. CPPs have a disproportionately larger number of positively charged residues—especially arginines—and hydrophobic residues—such as leucines. To better understand how CPPs differ from other peptides we used a data set of 109 CPPs (average length, 18 amino acids; average net charge, +4.8) and of 1000 15-mer peptides obtained by randomly selecting peptide sequences from a collection of approximately 20 000 human protein sequences. For these peptides we calculated two physical–chemical properties—polarity (PP1) and hydrophobicity (PP2)—which are scaled principal component scores that summarize a broad set of descriptors calculated based on the interaction of each amino acid residue with several chemical groups (or “probes”), such as charged ions, methyl, hydroxyl groups, and so forth, as described by Cruciani et al.¹⁵ The probes reflect a broad range of chemical groups that amino acid residues may encounter in a biological system. PP1 and PP2 were defined for individual amino acid residues (Figure 1A, SI Table 1). To calculate PP1 and PP2 of each peptide we calculated the average PP1 and PP2 of all the amino acids in the corresponding peptide sequence.

As shown in Figure 1B, randomly generated peptides and CPPs occupy distinct regions of the PP1/PP2 space. CPPs disproportionately occupy the area H colored in green (43% of CPPs vs 1% of random peptides occupy this space), suggesting that peptide sequences with an amino acid composition that falls into this area have a significantly increased likelihood of being cell-penetrating (Figure 1C). Using this classification scheme, R9 possesses high hydrophobicity due to the long

carbon chain but also high polarity due to the positive charge. As a further comparison, the well-established penetratin CPP is relatively hydrophobic with intermediate polarity.

We designed a collection of cell-penetrating peptides starting from peptide sequences of varying length (5–15 amino acids) that fall into the region H of the PP1-PP2 space (Table 1,

Table 1. Cell-Penetrating Peptides for the First Round of Testing^a

abbreviation	sequence	type
L1	Fluo- MIIIIIGSTS RDHMLHEYVNAAGIT-NH₂ ^b	linear
L2	Fluo- FLLIRRVLGSTS RDHMLHEYVNAAGIT-NH₂	linear
L3	Fluo- PWPRVPWRWGSTS RDHMLHEYVNAAGIT-NH₂	linear
L4	Fluo- LKRAIWLIKGSTS RDHMLHEYVNAAGIT-NH₂	linear
L5	Fluo- FRWLFRLLFRGSTS RDHMLHEYVNAAGIT-NH₂	linear
C1	Fluo- FIDLKRIKIWLICK-NH₂ ^c	cyclic
C2	Fluo- YLKFIPLKDAIWKIK-NH₂	cyclic
R9	Fluo- RRRRRRRRRGSTS RDH(Nle) VLHEYVNAAGIT-Ado-NH₂ ^d	linear

^aThe CPP domains are printed in bold face. The short linear CPPs are conjugated to the 11th strand of the GFP protein via a GSTS spacer.

^bFluo refers to an N-terminal carboxyfluorescein, NH₂ to a C-terminal amidation. ^cThe side chains of the underlined residues are linked by a lactam bridge. ^dAdo: 8-amino-3,6-dioxaoctanoic acid.

Figure 2A). These peptide sequences were extracted from proteins included in the UNIPROT database. MIILII (L1) was derived from MILLII, which corresponds to one of the transmembrane motifs of Aquaporin 9 (aa 170–175); FLLIRRVL (L2) was derived from YLLIRRVL, which corresponds to the transmembrane region of the Antigen peptide transporter 2 protein (aa 376–383); PWPRVPWRW (L3) corresponds to a fragment of the signal peptide of Emilin-2 (aa 7–15)—signal peptides direct nascent proteins into their correct subcellular localization and due to their hydrophobic nature they have been found as a source of CPPs; similarly, FRWLFRLLFR (L5) is a fragment of a signal peptide of the *Cronobacter* Bifunctional Protein Aas (aa 6–15); YLKFIPLKDAIWKIK (C2) was derived by cyclization of YLKFIPLKRAI-WLIK, which was selected from a fragment of *Saccharomyces*

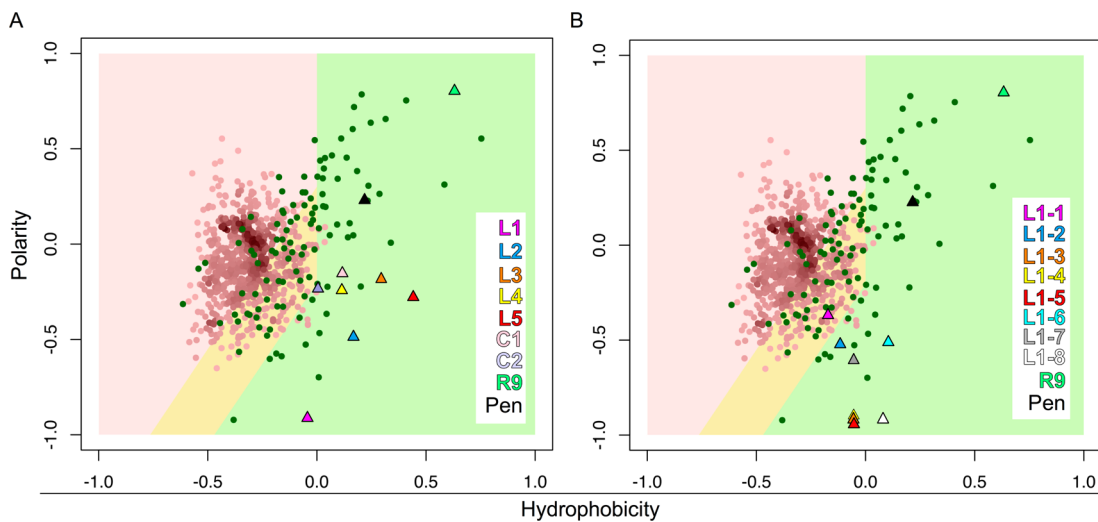


Figure 2. Properties of the designed CPPs of the first collection (A) and the second collection (B). Properties were calculated based the bold face sequences in Tables 1 and 2. Residues involved in lactam bridge formation were replaced by glutamine and asparagine, norleucine by leucine.

cerevisiae mediator of RNA polymerase II transcription subunit 12 (aa 161–176); LKRAIWLIK (L4) is a derivative of YLKFIPLKRAIWLIK; last, FIDLKRKIWLK (C1) was derived by cyclization of L4.¹⁶ These peptides were selected to explore how extreme ranges of properties might affect cellular uptake. For example, we incorporated a very short CPP (L1), and analogues of linear and cyclic CPPs (L4, C1, C2).

In order to validate their capacity as vectors for cellular peptide import, the linear peptides were C-terminally elongated with a 4-amino-acids GSTS-spacer followed by a 16-amino-acids peptide corresponding to the 11th strand of the enhanced GFP protein. This 16-mer peptide has a net charge of -1 and little hydrophobicity, and therefore it should not promote uptake. Elongation with this moiety shifts the peptides into the less hydrophobic and more polar region of parameter space out of the region populated by CPPs (SI Figure 1)

Cytosolic delivery of this peptide into cells transfected with a GFP fragment comprising the first ten strands of the GFP beta-barrel can be detected by a robust and sensitive reporter assay based on GFP complementation and formation of the fluorescent protein.^{13,14} For reasons of complexity during synthesis, the lactam-bridged cyclic peptides were tested without C-terminal elongation.

Cellular Uptake and Distribution. Except for one peptide (L5) all peptides were readily dissolvable in DMSO. The cellular uptake of the fluorescein-labeled peptides was investigated by flow cytometry and the subcellular distribution by confocal microscopy using HeLa cells (Figures 3 and 4). HeLa cells are a widely used cell model and therefore highly suitable for cross-referencing of results. Uptake was assessed in the absence and presence of serum. Serum has been recognized as an important factor in the uptake of CPPs and delivery vectors in general.¹⁷ On one hand, it can sequester peptide, and on the other hand, proteases present in serum can degrade peptide. Both mechanisms reduce the effective peptide concentration. We had observed that for nonaarginine for short-term incubations of about 30 min the presence of serum lowers the effective concentration by one-half. In the absence of serum, the apolar and highly hydrophobic hexapeptide MIILII showed the most effective uptake. However, it reached only about 13% of the uptake measured for R9 (Figure 3A). Uptake was detected also for the two lactam-bridged peptides, but to a

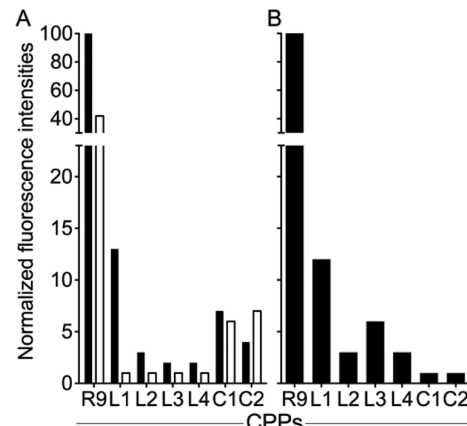


Figure 3. Normalized intracellular fluorescence intensities of analyzed carboxyfluorescein-labeled peptides. HeLa cells were incubated for (A) 30 min with 5 μ M in the presence (open bars) or 2 μ M CPP in the absence (closed bars) of fetal calf serum and for (B) 2 h with 2 μ M CPP in medium without serum and analyzed by flow cytometry for intracellular fluorescence. Before measuring, trypan blue (0.4% end concentration) was administered to quench cell surface-bound fluorescence and restrict the recorded signal to intracellular fluorescence.

lower degree. Interestingly, peptides L3 and L4 showed even less uptake, even though with the presence of arginine and tryptophan residues they conformed more strongly with structural characteristics of CPPs.

The sensitivity to serum differed greatly. Uptake of the linear hexapeptide was nearly eliminated completely in the presence of serum, while for the cyclopeptides serum had no impact at all. In the absence of serum, an extension of incubation time to 2 h had little impact on relative uptake efficiencies (Figure 3B). To validate that uptake was a characteristic of peptides falling into the green area of parameter space we also tested uptake of a collection of peptides from an earlier project addressing intracellular peptide stability. We also included the GFP11 motif to demonstrate that this peptide alone does not have the capacity to enter cells. These peptides corresponded to known interaction motifs with signal transduction motifs and intracellular stability required introduction by electroporation (SI

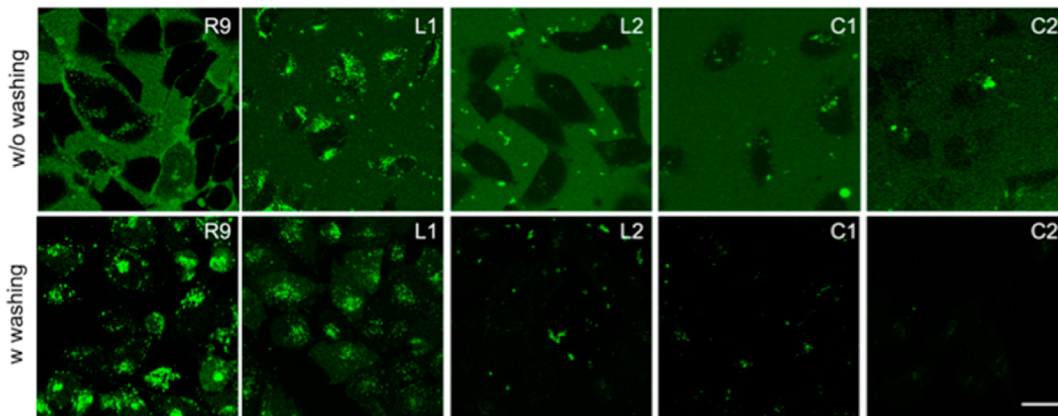


Figure 4. Live cell confocal microscopy for the determination of uptake and intracellular localization. HeLa cells were incubated with 2 μ M CPP in the absence of fetal calf serum and analyzed by confocal microscopy regarding uptake efficiency and localization after 2 h. After washing, trypan blue was administered to quench extracellular and cell surface-bound fluorescence. Bar, 20 μ m.

Table 2).¹⁸ Except for one very polar peptide, these peptides mapped into the non-CPP area of the parameter space (SI Figure 2). At the concentration of 20 μ M GFP11 had a cell associated fluorescence of only 3.7% in comparison to R9. For the collection of control peptides, the maximum cell-associated fluorescence was 3% of the one of R9 (SI Figure 3).

To assess the subcellular distribution, confocal microscopy was performed before washing of cells and after washing in the presence of trypan blue. In this way we aimed to first capture potential accumulation and aggregation of peptides at the plasma membrane and second to restrict detection to only intracellular fluorescence. Even for the very hydrophobic hexapeptide there was no indication of membrane enrichment. All peptides showed primarily punctate intracellular fluorescence indicative of endocytic uptake (Figure 4).

Testing of Conformationally Constrained Hydrophobic Peptides. Considering the activity of the hydrophobic and conformationally constrained peptides, in a second round we set out to explore combinations of both structural characteristics. Lactam bridges were incorporated into highly hydrophobic, nonpolar sequences. In addition, we incorporated single D-amino-acid substitutions and nonproteinogenic amino acids as a further means to prevent proteolysis (Table 2). A peptide sequence (L1–6) which was reported as capable of spontaneous cell membrane permeability was also included.¹⁹ In comparison to the first collection, this second one was more biased toward the nonpolar parameter space (Figure 2B, SI Figure 1). All peptides were C-terminally extended with an optimized GFP11 domain to detect cytosolic delivery using the GFP complementation assay.¹³ This peptide differs from the original one by an isosteric methionine to norleucine substitution and a C-terminal extension with a short polyethylene glycol building block.

With the exception of one purely hydrophobic D-peptide (L1–8) which could not be dissolved, peptides were tested for uptake and intracellular distribution. For uptake in HeLa cells, one lactam-bridged, fully hydrophobic peptide (L1–7) reached about 40% of the uptake of R9 and two more about 15% demonstrating an increase in overall activity (Figure 5).

This time we extended our analyses to two more cell lines. Next to HeLa cells we also included HEK and Jurkat cells. For arginine-rich CPPs HEK cells had shown a concentration-independent homogeneous cytoplasmic distribution of fluorescence indicating a direct translocation of the plasma

Table 2. Peptides to Test the Role of Conformationally Constrained Hydrophobic Motifs for Cell-Penetrating Capacity

abbreviations	sequences
L1–1	Fluo- <u>KIIIIDGTSRDH(Nle)</u> VLHEYVNAAGIT-Ado-NH ₂ ^a
L1–2	Fluo- <u>KNleIIIIDGTSRDH(Nle)</u> VLHEYVNAAGIT-Ado-NH ₂
L1–3	Fluo-Nle <u>IIILIGSTS RDH(Nle)</u> VLHEYVNAAGIT-Ado-NH ₂
L1–4	Fluo-m <u>IliIIGSTS RDH(Nle)</u> VLHEYVNAAGIT-Ado-NH ₂
L1–5	Fluo-MIILIIMGVADLIKKFESISKEE-NH ₂
L1–6	Fluo-PLILLRLLLRGSTS RDH(Nle)VLHEYVNAAGIT-Ado-NH ₂
L1–7	Fluo-F <u>IIIIKKILLIGSTS RDH(Nle)</u> VLHEYVNAAGIT-Ado-NH ₂
L1–8	Fluo-f <u>iiiliGSTS RDH(Nle)</u> VLHEYVNAAGIT-Ado-NH ₂
R9	Fluo-R <u>RRRRRRRRRGSTS RDH(Nle)</u> VLHEYVNAAGIT-Ado-NH ₂

^aFluo refers to an N-terminal carboxyfluorescein, NH₂ to a C-terminal amidation, Ado to 8-amino-3,6-dioxo-octanoic acid. The side chains of the underlined residues are linked by a lactam bridge. Peptide L1–5 was extended by a random sequence instead of GFP11.

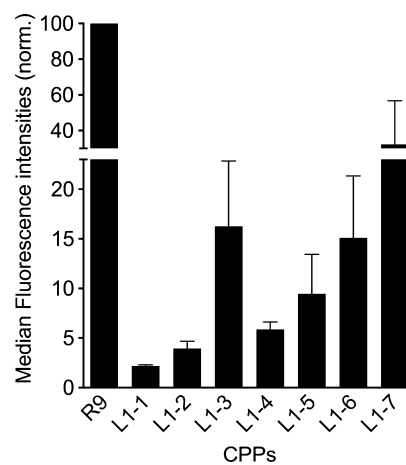


Figure 5. Relative uptake efficiencies of the second peptide collection. Uptake was normalized to uptake of the Fluo-R9 conjugate. HeLa cells were incubated with the indicated peptides at a concentration of 2 μ M for 2 h in serum-free medium. Error bars represent standard errors of the mean (SEM) of three independent experiments.

membrane as a mechanism of uptake.¹³ Jurkat cells were included as a suspension cell line.

In this case the most effective peptide in all three cell lines was a linear hydrophobic peptide with two arginine residues at a three residues spacing (L1–6). After 24 h long-term incubation for this peptide more fluorescence was retained inside the cell than for nonaarginine. The higher activity of L1–7 was restricted to HeLa cells at low concentrations (Figure 6).

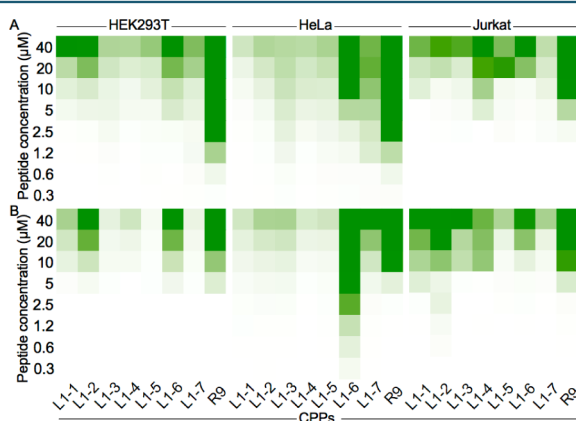


Figure 6. Uptake of conformationally constrained and hydrophobic CPPs in HEK, HeLa, and Jurkat cells. Uptake was assessed (A) after a 2 h incubation in the absence of serum and (B) after a 24 h incubation in the presence of serum. The values are averages of two independent experiments. Green reflects high, white low uptake.

Since cells were coincubated with propidium iodide as a marker for compromised membrane integrity the flow cytometry measurements also enabled an assessment of toxicity. At a concentration of 20 μM and 2 h incubation in the absence of serum membrane integrity was maintained to larger than 90% (SI Figure 4).

The intracellular distribution revealed a striking difference between HeLa and HEK cells. While in HeLa cells fluorescence was heterogeneously distributed throughout the cells, indicative of sequestration in endolysosomal compartments, in HEK cells a major part of the fluorescence was distributed homogeneously throughout the cytoplasm and nucleus. These differences that already became apparent after 2 h (SI Figure 5) were even more prominent after 24 h (Figure 7). After 24 h the signal for L1–6 was more intense than the one for R9.

Cytoplasmic Delivery of a Functional Peptide. Finally, we were interested to learn whether the cytoplasmic fluorescence reflected the presence of a functional peptide.

For this purpose, we employed the detection of GFP complementation. We restricted ourselves to the CPPs L1–2 and L1–6 which had shown high uptake efficiency in combination with cytosolic staining in HEK293 cells (Table 3).

Table 3. Peptides to Test for GFP Complementation

abbreviation	sequences
L1–2 Ac	Ac-K(Nle)IILIDGSTS RDH(Nle)VLHEYVNAAGIT-Ado-NH ₂ ^a
L1–6 Ac	Ac-PLILLRLRGSTS RDH(Nle)VLHEYVNAAGIT-Ado-NH ₂
R9	Ac-RRRRRRRRRGSTS RDH(Nle)VLHEYVNAAGIT-Ado-NH ₂

^aAc refers to an N-terminal acetylation, NH₂ to a C-terminal amidation, Nle to norleucine, and Ado to 8-amino-3,6-dioxo-octanoic acid. The side chains of the underlined residues are linked by a lactam bridge, Nle refers to a norleucine residue.

L1–6 yielded a clearly detectable GFP complementation and also L1–2 yielded some GFP fluorescence (Figure 8). Still, the R9-conjugated peptide exceeded both. Overall, the degree of complementation fully reproduced the relative uptake efficiencies observed for the fluorescein-labeled peptides demonstrating that the cell-associated fluorescence directly correlated to the amount of intact peptide present in the cytosol.

DISCUSSION

Here, we predicted and validated CPPs based on average side chain polarity and hydrophobicity as descriptors. First we showed that known CPPs preferably populate a region that is distinct from the one populated by the majority of randomly generated peptides in this two-dimensional parameter space.

For a collection of peptides that comprised short hydrophobic sequences as well as cationic amphipathic peptides, we surprisingly identified a purely hydrophobic peptide of only six amino acids as the most active peptide. We then generated a collection of analogs from this initial sequence which yielded a further increase in activity by up to a factor of 3. Next to nonaarginine we included a further previously published, but so far little explored sequence (L1–6) for further referencing. This peptide was identified by screening peptides from a highly biased random library, in which either arginine, lysine, or a hydrophobic residue was permitted at the various positions. The assay was designed in a way that only water-soluble peptides with the ability to enter liposomes by passive diffusion and that did not show membrane-disruptive behavior were selected. To determine the degree of bias of this collection, we

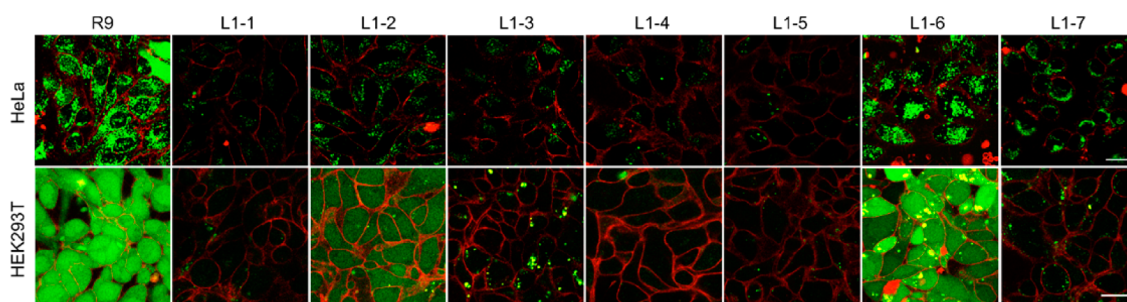


Figure 7. Subcellular distribution of CPPs. HeLa cells and HEK cells were incubated with the indicated peptides at a concentration of 20 μM in the presence of serum for 24 h. Following washing, cells were imaged in the presence of trypan blue to quench cell-associated fluorescence. Fluorescence from trypan blue is displayed as a red signal outside the cells. Bars, 20 μm.

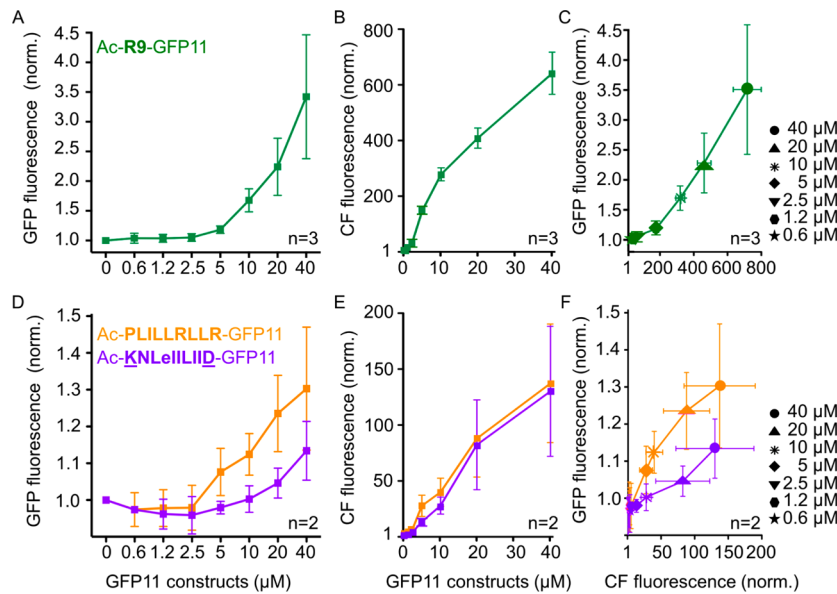


Figure 8. GFP complementation and correlation to cytosolic concentration of the GFP11 variants. (A,D) Fluorescence for both mCherry and GFP was detected by flow cytometry from morphologically intact cells gated based on forward versus sideward scatter after 2 h incubation with peptides in FCS-free medium. The GFP fluorescence for cells was normalized to the background signal acquired from mock-treated cells. Curves indicate the average of the normalized medians of (A) three and (D) two independent experiments. Error bars denote the standard error of the mean (SEM). (B,E) Dose response curve for the fluorescein-labeled counterparts representing the concentration-dependent increase of the carboxyfluorescein signal in the cytosol. (C,F) Correlation of the dose-dependent increase of GFP fluorescence and cell-associated carboxyfluorescein signal obtained from the respective pairs of samples.

plotted all 10 368 peptides into the parameter space. All peptides fell into the CPP-enriched region (SI Figure 6).

Uptake efficiencies were determined for peptides conjugated to a 16-amino-acids cargo peptide which strongly affected the bulk properties of the peptides (SI Figure 1). In most cases, CPPs are tested with a fluorophore as cargo only, which severely limits the relevance of the findings in contrast to our approach.

Cyclization by lactam bridge formation and incorporation of D-amino-acids benefited uptake in only some cases. Both modifications should increase peptide stability. Nevertheless, in our case, linear peptides were the most active ones, in contrast to previous reports on beneficial aspects of cyclization.^{5,20}

For the second peptide collection, uptake was measured for two adherent cell lines (HEK293T, HeLa) and one suspension cell line (Jurkat). Two peptides, L1–6 (PLILLRLLR) and R9, showed activity in all cell lines; the cyclic peptide L1–2 (CPP K(Nle)IIIID) had activity in HEK293T and Jurkat cells while L1–4 (mIiLII) only showed activity in Jurkat cells. Cell line preferences of CPPs have been reported before.²¹ However, the molecular basis of these differences is not clear.

After a 24 h incubation L1–6 (PLILLRLLR) showed even a higher cell-associated fluorescence than R9. Earlier we had observed that for nonarginine only little cell-associated fluorescence remained after long-term incubation, likely due to proteolytic degradation and cellular release of fluorescein labeled fragments.⁵

In HEK293T and Jurkat cells uptake of the cyclic peptide L1–2 (KNleIIIID) was higher than that of its linear analog L1–3 (NleIILII). However, there was no gain in relative uptake efficiency over time, indicating that most likely this higher uptake was not due to an increased stability but rather due to structural characteristics. A difference that may well be attributed to stability is the higher retention of L1–4 (mIiLII)

which incorporates two D-amino-acids in comparison to L1–5 (MIIILII) in HEK293T and Jurkat cells.

Endosomal sequestration is a major concern in the application of CPPs. In HeLa cells, staining was punctate in all cases, independent of incubation time, in line with uptake by endocytosis. Also, for L1–6 direct membrane permeation, as published before, was only observed for HEK but not for HeLa cells demonstrating that this route of import is a function of cell type and not a general characteristic.

Next to L1–6, in HEK293T cells also L1–2 yielded a diffuse cytosolic distribution and absence of punctate staining independent of incubation time. This observation suggests that these peptides enter the cytoplasm by direct crossing of the plasma membrane and not by endocytosis followed by endosomal release. For both peptides, the presence of intact peptide inside the cytosol was confirmed by the formation of fluorescent GFP using a complementation assay. This finding demonstrates that these eight/nine amino acid peptides had the capacity to carry a nonhydrophobic peptide of twice the size across the plasma membrane.

As a next step it will be highly interesting to investigate the *in vivo* distribution of these peptides. Polycationic CPPs show a propensity to accumulate in the liver and kidney.²² If this was not the case for these new CPPs, a further exploration in combination with targeting ligands may be highly interesting.²³ In this case, the targeting ligand would guide the localization while the CPP would drive uptake.

Following the work by Hällbrink et al., which was then also applied to the prediction of CPPs with intrinsic biological activity, this contribution is the second example of a successful prediction of CPPs using a descriptor set of accumulated side chain properties.²⁴ Nevertheless, our results also show the limitations of this approach. Within the peptide collection the most active one could only be identified by an empirical approach. Also, the cell line dependence and uptake mechanism

cannot be predicted at this point. Here, more research will be needed to better understand the interplay of molecular and cellular descriptors. Candidates for cellular descriptors are the composition of the glycocalyx, the lipid composition, and the presence of certain endosomal pathways.²⁵

MATERIALS AND METHODS

Cell Culture. HeLa (DSMZ) and Jurkat E6.1 leukemia cells (ATCC) were maintained in RPMI 1640 and HEK293T cells (DSMZ) in DMEM (Gibco, Invitrogen, Eugene, OR, USA), respectively, supplemented with 10% fetal calf serum (FCS; PAN Biotech, Aidenbach, Germany). All cells were incubated at 37 °C in a 5% CO₂-containing, humidified incubator. Cells were passaged every 2 to 3 days. For detachment of adherent cells phosphate-buffered saline (PBS) containing 2 mM EDTA was used.

Peptides. Peptides extended by a nonaarginine moiety were purchased as C-terminal peptide amides from EMC micro-collections (Tübingen, Germany). The N-terminus was either capped by acetylation or by a carboxyfluorescein moiety. All other peptides were synthesized by Fmoc-strategy on an automated CS336 synthesizer. Carboxyfluorescein was attached on the resin using DIC/HOBt as coupling reagent. Peptides were purified by reversed phase HPLC using water/ACN (0.1% TFA) gradients to >95% purity. Lyophilization gave the final peptide as TFA salt. Stock solutions were prepared in DMSO in concentrations of 3–5 mM. Peptide concentrations were determined by measuring the absorption of the fluorescein moiety in 100 mM in Tris/HCl buffer pH 8.8, assuming a molar extinction coefficient for fluorescein $\epsilon_{492} = 75\,000 \text{ L/(mol} \times \text{cm)}$. For unlabeled peptides concentrations were determined based on weight and molecular mass.

Transfection with GFP1–10. HEK293T cells were seeded in 48-well plates for flow cytometry with 40 000 cells in DMEM with FCS (10%) and cultured overnight at 37 °C, 5% CO₂. The next day, the culture medium was replaced and cells were transfected with mCherry-GFP1–10 plasmid via lipofectamine 2000 (Invitrogen, Eugene, U.S.A.) under adherent condition.¹³ After 24 h, the medium was replaced by fresh culture medium containing 10% FCS and the cells were cultured overnight.

Flow Cytometry. For detection of GFP complementation flow cytometry was performed on a CyAn ADP flow cytometer (Beckman Coulter, Woerden, The Netherlands) using spectral ranges 530/40 for GFP and 613/20 for mCherry. A BD FACSCalibur (BD Biosciences, Erembodegem, Belgium) flow cytometer with a 488 nm argon ion laser was used for flow cytometry of cells incubated with carboxyfluorescein-labeled variants. FCS Express Version 5 Research Edition (De Novo Software, Los Angeles, CA) was used for the analysis of the generated data. Per sample, 10 000 morphologically intact cells were gated based on forward versus sideward scatter and analyzed.

CPP-Mediated Import of GFP11 Variants. The medium was replaced by RPMI 1640 for adherent HeLa and Jurkat E6.1 leukemia suspension cells or by 150 μL DMEM for adherent HEK293T cells. For incubation over 24 h, the medium was supplemented with 10% FCS. Peptides were administered at the indicated concentrations by adding a 150 μL premix. Cells were detached using PBS containing 2 mM EDTA (HeLa and HEK293T), transferred into tubes, and flow cytometry was performed.

Confocal Microscopy. Cells were seeded in 8-well microscopy chambers (IBIDI, München, Germany) with

40 000 cells per well in DMEM with FCS (10%) and cultured overnight at 37 °C, 5% CO₂. The next day, medium of the cells was replaced by 150 μL RPMI 1640 (HeLa) or DMEM (HEK293T) without phenol red and FCS. Cell culture medium containing the indicated concentrations of peptide was prepared as premix and transferred to the IBIDI 8-well microscopy chambers. Confocal images were acquired 2 h after peptide administration. To study the peptide mediated import of the CPPs of the first round, confocal microscopy was performed on a TCS SP5 confocal microscope (Leica Microsystems, Mannheim, Germany) equipped with an HCX PL APO 63× 1.2 N.A. water immersion lens. Carboxyfluorescein fluorescence was excited using the 488 nm line of an argon ion laser and fluorescence detected at 500–550 nm. Confocal pictures for the study of CPPs of the second round were taken on a TCS SP8 confocal microscope (Leica Microsystems, Mannheim, Germany) equipped with an HCX PL APO 63× 1.2 N.A. water immersion lens after 2 or 24 h of incubation with peptides. Carboxyfluorescein fluorescence was excited using the 488 nm line of a white laser (WLL) and fluorescence detected at 500–550 nm. Trypan blue was excited using the 568 nm line of the WLL and fluorescence detected at 600–660 nm.

ASSOCIATED CONTENT

S Supporting Information

The Supporting Information is available free of charge on the ACS Publications website at DOI: [10.1021/acs.bioconjchem.6b00535](https://doi.org/10.1021/acs.bioconjchem.6b00535).

Supplemental data providing further information on the principal properties of amino acids (Table 1), properties of the designed CPPs including GFP11 (Figure 1) and of the control peptides (Figure 2), uptake of control peptides (Figure 3), maintenance of membrane integrity for peptides of the second collection (Figure 4), uptake of the peptides of the second collection at 10 μM after 2 h (Figure 5), and properties of the biased peptide collection through which peptide L1–6 was identified (Figure 6) ([PDF](#))

R-code to calculate peptide properties ([ZIP](#))

AUTHOR INFORMATION

Corresponding Author

*E-mail: francesca.milletti@roche.com.

ORCID

Roland Brock: [0000-0003-1395-6127](https://orcid.org/0000-0003-1395-6127)

Notes

The authors declare no competing financial interest.

ACKNOWLEDGMENTS

This work was supported by the Roche postdoc programme (RPF 272).

REFERENCES

- (1) Milletti, F. (2012) Cell-penetrating peptides: classes, origin, and current landscape. *Drug Discovery Today* 17, 850–860.
- (2) Mitchell, D. J., Kim, D. T., Steinman, L., Fathman, C. G., and Rothbard, J. B. (2000) Polyarginine enters cells more efficiently than other polycationic homopolymers. *J. Pept. Res.* 56, 318–325.
- (3) Derossi, D., Joliot, A. H., Chassaing, G., and Prochiantz, A. (1994) The third helix of the Antennapedia homeodomain trans-

- locates through biological membranes. *J. Biol. Chem.* 269, 10444–10450.
- (4) Prochiantz, A. (1996) Getting hydrophilic compounds into cells: lessons from homeopeptides. *Curr. Opin. Neurobiol.* 6, 629–634.
- (5) Wallbrecher, R., Depre, L., Verdurmen, W. P., Bovee-Geurts, P. H., van Duinkerken, R. H., Zekveld, M. J., Timmerman, P., and Brock, R. (2014) Exploration of the design principles of a cell-penetrating bicyclic peptide scaffold. *Bioconjugate Chem.* 25, 955–964.
- (6) Saar, K., Lindgren, M., Hansen, M., Eiriksdottir, E., Jiang, Y., Rosenthal-Aizman, K., Sassian, M., and Langel, U. (2005) Cell-penetrating peptides: a comparative membrane toxicity study. *Anal. Biochem.* 345, 55–65.
- (7) Fischer, D., Li, Y., Ahlemeyer, B., Kriegstein, J., and Kissel, T. (2003) In vitro cytotoxicity testing of polycations: influence of polymer structure on cell viability and hemolysis. *Biomaterials* 24, 1121–1131.
- (8) Lin, Y.-Z., Yao, S., Veach, R. A., Torgerson, T. R., and Hawiger, J. (1995) Inhibition of nuclear translocation of transcription factor NF- κ B by a synthetic peptide containing a cell membrane-permeable motif and nuclear localization sequence. *J. Biol. Chem.* 270, 14255–14258.
- (9) Fischer, R., Waizenegger, T., Köhler, K., and Brock, R. (2002) A quantitative validation of fluorophore-labelled cell-permeable peptide conjugates: Fluorophore and cargo dependence of import. *Biochim. Biophys. Acta, Biomembr.* 1564, 365–374.
- (10) Hällbrink, M., Kilk, K., Elmquist, A., Lundberg, P., Lindgren, M., Jiang, Y., Pooga, M., Soomets, U., and Langel, Ü. (2005) Prediction of cell-penetrating peptides. *Int. J. Pept. Res. Ther.* 11, 249–259.
- (11) Sandberg, M., Eriksson, L., Jonsson, J., Sjöstrom, M., and Wold, S. (1998) New chemical descriptors relevant for the design of biologically active peptides. A multivariate characterization of 87 amino acids. *J. Med. Chem.* 41, 2481–2491.
- (12) van Asbeck, A. H., Beyerle, A., McNeill, H., Bovee-Geurts, P. H., Lindberg, S., Verdurmen, W. P., Hallbrink, M., Langel, U., Heidenreich, O., and Brock, R. (2013) Molecular Parameters of siRNA-Cell Penetrating Peptide Nanocomplexes for Efficient Cellular Delivery. *ACS Nano* 7, 3797–3807.
- (13) Schmidt, S., Adjobo-Hermans, M. J., Wallbrecher, R., Verdurmen, W. P., Bovee-Geurts, P. H., van Oostrum, J., Milletti, F., Enderle, T., and Brock, R. (2015) Detecting Cytosolic Peptide Delivery with the GFP Complementation Assay in the Low Micromolar Range. *Angew. Chem., Int. Ed.* 54, 15105–15108.
- (14) Milech, N., Longville, B. A., Cunningham, P. T., Scobie, M. N., Bogdawa, H. M., Winslow, S., Anastasas, M., Connor, T., Ong, F., Stone, S. R., et al. (2015) GFP-complementation assay to detect functional CPP and protein delivery into living cells. *Sci. Rep.* 5, 18329.
- (15) Cruciani, G., Baroni, M., Carosati, E., Clementi, M., Valigi, R., and Clementi, S. (2004) Peptide studies by means of principal properties of amino acids derived from MIF descriptors. *J. Chemom.* 18, 146–155.
- (16) Magzoub, M., Oglecka, K., Pramanik, A., Goran Eriksson, L. E., and Graslund, A. (2005) Membrane perturbation effects of peptides derived from the N-termini of unprocessed prion proteins. *Biochim. Biophys. Acta, Biomembr.* 1716, 126–136.
- (17) Kosuge, M., Takeuchi, T., Nakase, I., Jones, A. T., and Futaki, S. (2008) Cellular internalization and distribution of arginine-rich peptides as a function of extracellular peptide concentration, serum, and plasma membrane associated proteoglycans. *Bioconjugate Chem.* 19, 656–664.
- (18) Ruttekolk, I. R., Witsenburg, J. J., Glauner, H., Bovee-Geurts, P. H., Ferro, E. S., Verdurmen, W. P., and Brock, R. (2012) The intracellular pharmacokinetics of terminally capped peptides. *Mol. Pharmaceutics* 9, 1077–1086.
- (19) Marks, J. R., Placone, J., Hristova, K., and Wimley, W. C. (2011) Spontaneous membrane-translocating peptides by orthogonal high-throughput screening. *J. Am. Chem. Soc.* 133, 8995–9004.
- (20) Lattig-Tunnemann, G., Prinz, M., Hoffmann, D., Behlke, J., Palm-Apergi, C., Morano, I., Herce, H. D., and Cardoso, M. C. (2011) Backbone rigidity and static presentation of guanidinium groups increases cellular uptake of arginine-rich cell-penetrating peptides. *Nat. Commun.* 2, 453.
- (21) Mueller, J., Kretzschmar, I., Volkmer, R., and Boisguerin, P. (2008) Comparison of cellular uptake using 22 CPPs in 4 different cell lines. *Bioconjugate Chem.* 19, 2363–2374.
- (22) Sarko, D., Beijer, B., Garcia Boy, R., Nothelfer, E. M., Leotta, K., Eisenhut, M., Altmann, A., Haberkorn, U., and Mier, W. (2010) The pharmacokinetics of cell-penetrating peptides. *Mol. Pharmaceutics* 7, 2224–2231.
- (23) Cheng, C. J., and Saltzman, W. M. (2011) Enhanced siRNA delivery into cells by exploiting the synergy between targeting ligands and cell-penetrating peptides. *Biomaterials* 32, 6194–6203.
- (24) Jones, S., Holm, T., Mager, I., Langel, U., and Howl, J. (2010) Characterization of bioactive cell penetrating peptides from human cytochrome c: protein mimicry and the development of a novel apoptogenic agent. *Chem. Biol.* 17, 735–744.
- (25) Favretto, M. E., Wallbrecher, R., Schmidt, S., van de Putte, R., and Brock, R. (2014) Glycosaminoglycans in the cellular uptake of drug delivery vectors - Bystanders or active players? *J. Controlled Release* 180, 81–90.

**Identification of short hydrophobic CPPs for cytosolic peptide delivery by
rational design**

Samuel Schmidt,[§] Merel J. W. Adjobo-Hermans,[§] Robin Kohze,[§] Thilo Enderle,[†]
Roland Brock,[§] Francesca Milletti^{*,‡}

[§] Department of Biochemistry (286), Radboud Institute for Molecular Life Sciences,
Radboud University Medical Center, Geert Grooteplein 28, 6525 GA Nijmegen, The
Netherlands

[†] Roche Pharmaceutical Research and Early Development, Roche Innovation Center
Basel, Grenzacherstrasse 124, 4070 Basel, Switzerland

[‡] Roche Pharmaceutical Research and Early Development, Roche Innovation Center
New York, 430 East 29th Street, 10016 New York, NY

* E-mail: francesca.milletti@roche.com

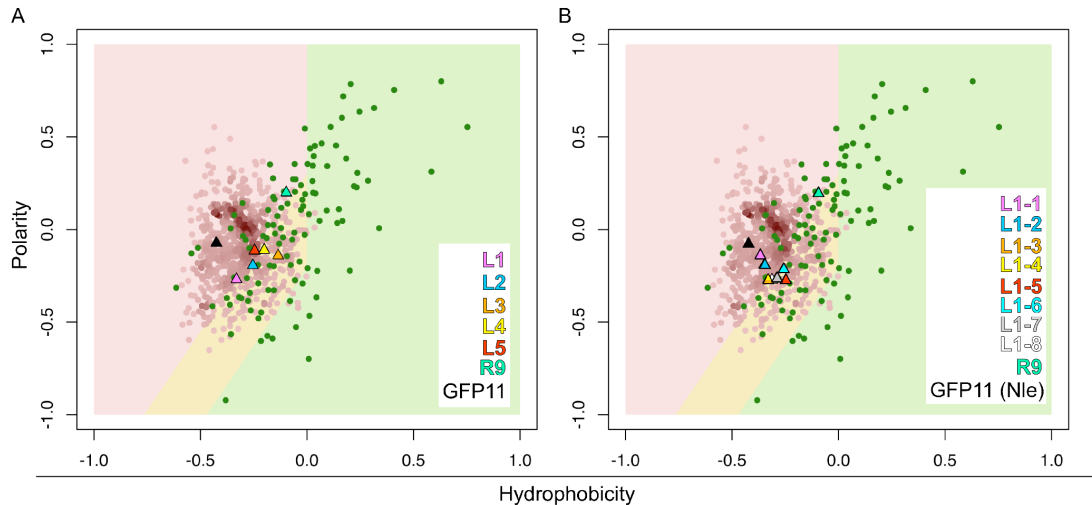
Supporting Information

Table of contents

	Page
Supplemental Table 1: Principal properties of amino acids as reported by Cruciani et al. (2004) ¹	2
Supplemental Figure 1: Properties of the designed CPPs including GFP11	3
Supplemental Table 2: Control peptides to test for uptake of peptides with non-CPP characteristics.	3
Supplemental Figure 2: Properties of the control peptide collection	4
Supplemental Figure 3: Uptake of peptides with non-CPP characteristics	4
Supplemental Figure 4: Maintenance of membrane integrity	5
Supplemental Figure 5: Uptake of the second collection after 2 h	5
Supplemental Figure 6: Properties of the biased peptide library by Marks et al. ²	6
R-code to calculate peptide properties – downloadable zip-folder	

Supplemental Table 1. Principal properties of amino acids as reported by Cruciani et al.

Amino acids		Polarity	Hydrophobicity
1-letter	3-letter	PP1	PP2
A	Ala	-0.96	-0.76
R	Arg	0.80	0.63
N	Asn	0.82	-0.57
D	Asp	1.00	-0.89
C	Cys	-0.55	-0.47
E	Glu	0.94	-0.54
Q	Gln	0.78	-0.30
G	Gly	-0.88	-1.00
H	His	0.67	-0.11
I	Ile	-0.94	-0.05
L	Leu	-0.90	0.03
K	Lys	0.60	0.10
M	Met	-0.82	0.03
F	Phe	-0.85	0.48
P	Pro	-0.81	-0.40
S	Ser	0.41	-0.82
T	Thr	0.40	-0.64
W	Trp	0.06	1.00
Y	Tyr	0.31	0.42
V	Val	-1.00	-0.43

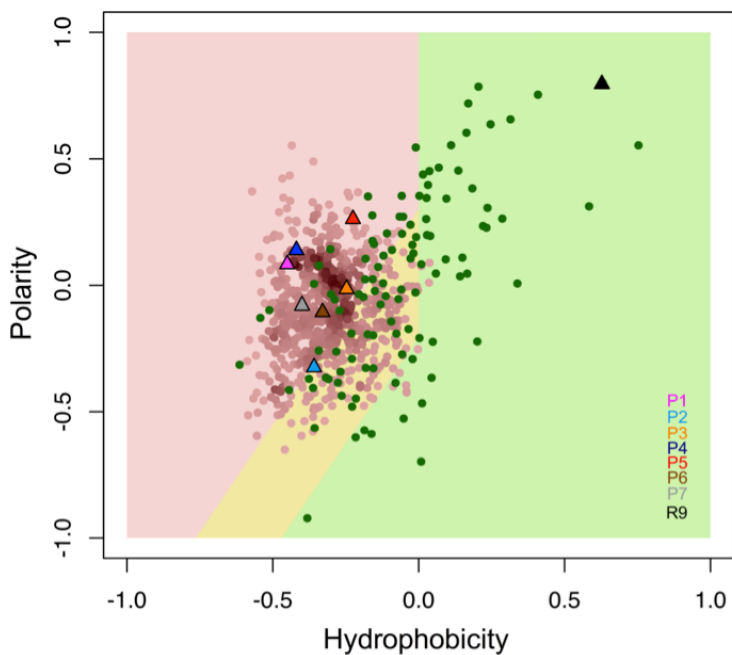


Supplemental Figure 1. Properties of the designed CPPs including GFP11 of the first collection (A) and the second collection (B). Properties were calculated based the complete peptide sequences including GSTS-GFP11 (A) or GFP11 (Nle) (B) in tables 1 and 2 except for peptide L1-5 which was elongated by a random sequence. Residues involved in lactam bridge formation were replaced by glutamine and asparagine, norleucine by leucine.

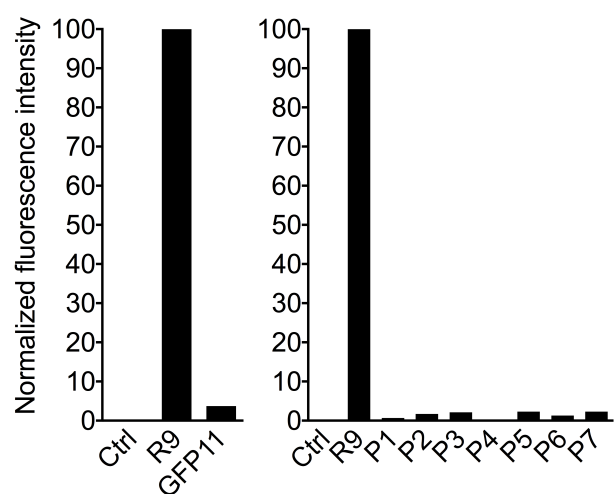
Supplemental Table 2. Peptides with non-CPP characteristics as published previously in Ruttekolk et al.³

Abbr.	Sequences
Fluo-GFP11	Fluo-GSTS RDH(Nle) VLHEYVNAAGIT-Ado-NH ₂ *
P1	Fluo-Ahx-ptsdplvvlygpnhyddede-NH ₂
P2	Fluo-Ahx-laamprqppvppqqptkgs-NH ₂
P3	Fluo-Ahx-QPPP VNRNLKPDRKAKPTPLD- NH ₂
P4	Fluo-Ahx-EASLDGSRE(pY)VNVSQEL-NH ₂
P5	Fluo-Ahx-NQL(pY)NELNLGRREE(pY)DV-NH ₂
P6	Fluo-Ahx-LDIQDKPPAPP MRNT-NH ₂
P7	Fluo-Ahx-KSTGSVD(pY)LALDFQPS-NH ₂

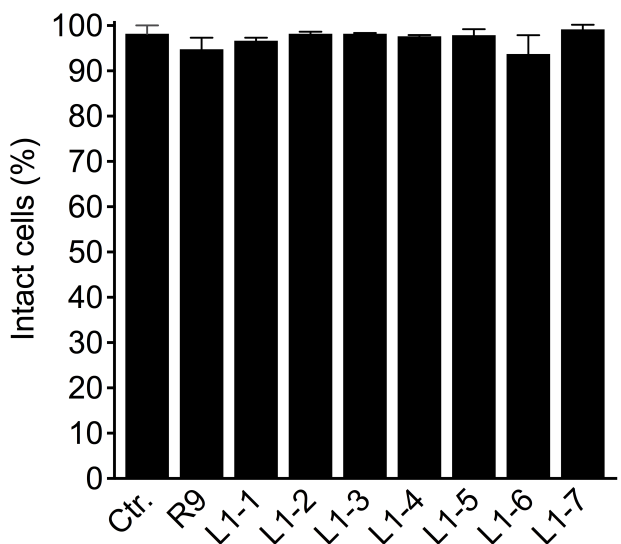
*Fluo refers to an N-terminal carboxyfluorescein, NH₂ to a C-terminal amidation, Nle to norleucine, Ado to 8-amino-3,6-dioxo-octanoic acid, Ahx to amino hexanoic acid, lower case letters indicate D-amino acids, pY phosphotyrosine.



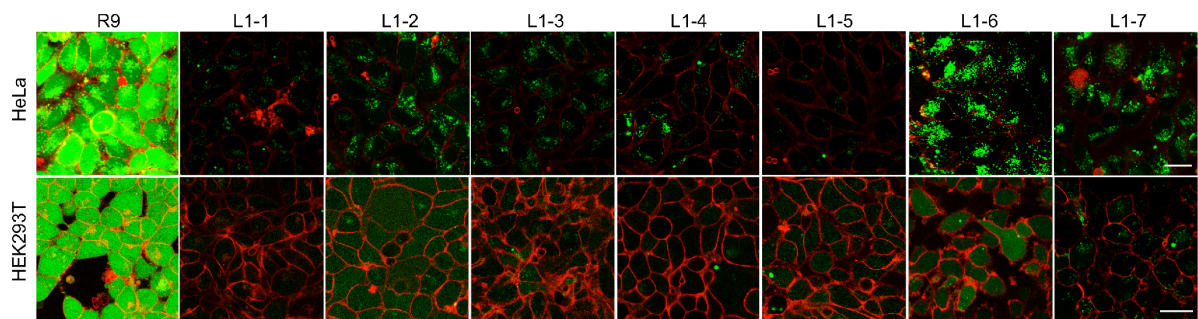
Supplemental Figure 2. Properties of the control collection of peptides with non-CPP characteristics. Phosphotyrosine was replaced by tyrosine.



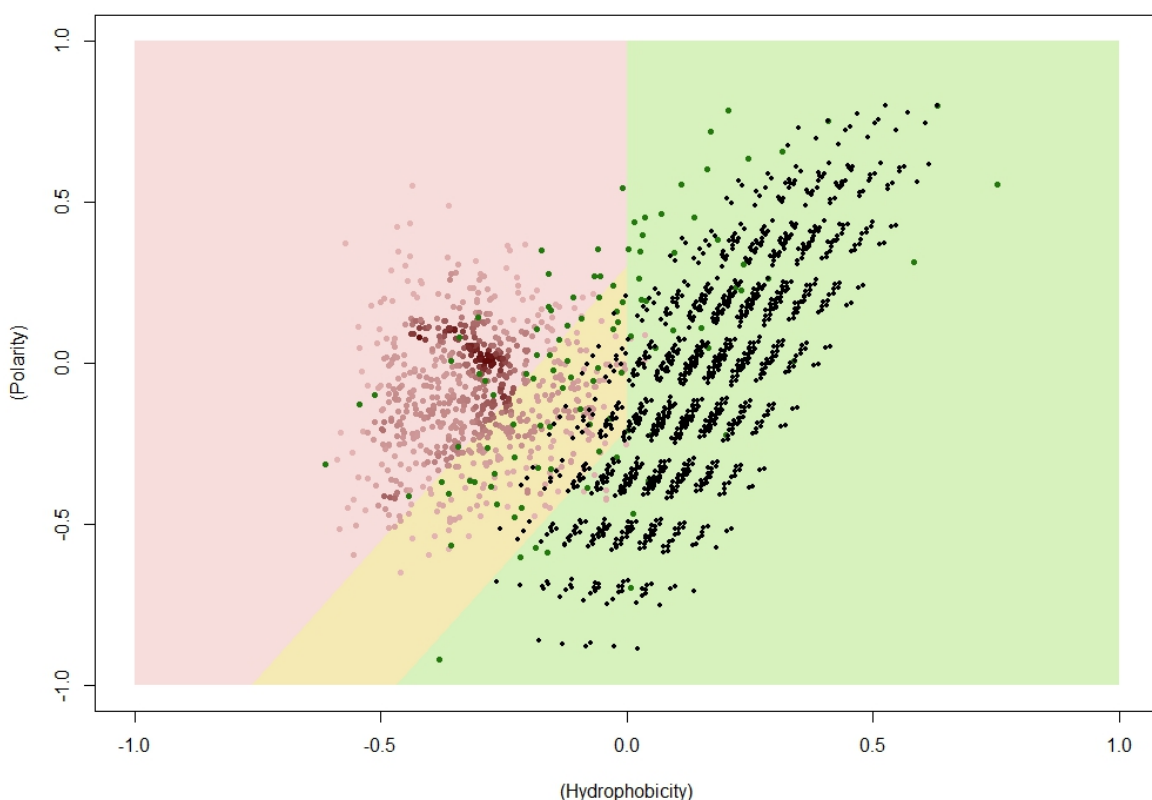
Supplemental Figure 3. Uptake of peptides with non-CPP characteristics into HEK cells. Cells were incubated with 20 μ M of peptides for 2 h in serum-free medium. Cell-associated fluorescence was determined by flow cytometry in the presence of trypan blue.



Supplemental Figure 4. Maintenance of membrane integrity as determined by propidium iodide exclusion. Cells were incubated with the peptides at a concentration of 20 μ M for 2 h in the absence of serum. The error bars corresponds to the standard deviation, n=2.



Supplemental Figure 5. Uptake of CPPs of the second collection at 10 μ M in the absence of serum for 2 h. Following washing, cells were imaged in the presence of trypan blue to quench cell-associated fluorescence. Fluorescence from trypan blue is displayed as a red signal outside the cells. Bars, 20 μ m.



Supplemental Figure 6. Polarity versus hydrophobicity properties of the combinatorial peptide collection as described by Marks et al.²

Supplemental References

- (1) Cruciani, G., Baroni, M., Carosati, E., Clementi, M., Valigi, R., and Clementi, S. (2004) Peptide studies by means of principal properties of amino acids derived from MIF descriptors. *J. Chemometrics* 18, 146-155.
- (2) Marks, J. R., Placone, J., Hristova, K., and Wimley, W. C. (2011) Spontaneous membrane-translocating peptides by orthogonal high-throughput screening. *J. Am. Chem. Soc.* 133, 8995-9004.
- (3) Ruttekolk, I. R., Witsenburg, J. J., Glauner, H., Bovee-Geurts, P. H., Ferro, E. S., Verdurmen, W. P., and Brock, R. (2012) The intracellular pharmacokinetics of terminally capped peptides. *Mol. Pharm.* 9, 1077-1086.